Biosorption of cationic dyes by Pará chestnut husk (*Bertholletia excelsa*)

Jordana Georgin, Bianca Silva Marques, Enrique Chaves Peres, Daniel Allasia and Guilherme Luiz Dotto

ABSTRACT

Pará chestnut husk (*Bertholletia excelsa*) (PCH), an agro-industrial waste largely generated in Brazil, was employed as a low-cost and efficient biosorbent to remove the cationic dyes Crystal Violet (CV) and Methylene Blue (MB) from aqueous media. PCH presented an amorphous structure containing carboxylic acids, esters, ketones and aldehydes on the surface. Non-porous and irregular particles were also observed. For both dyes, the biosorption capacity was favored under acid conditions. Equilibrium was attained within 40 min at 25 °C with a PCH dosage of 0.5 g L^{-1}. The biosorption kinetic curves were satisfactory explained by the pseudo-first-order model. The Freundlich model was best for representing the equilibrium curves. The maximum biosorption capacities were 83.6 and 83.8 mg g^{-1} for CV and MB, respectively. PCH was efficient for treating a simulated textile effluent containing several dyes and chemicals, achieving a color removal of 90%. In this way, PCH can be considered as an option for treating colored effluents containing textile dyes.

Key words | biosorbent, cationic dyes, Pará chestnut husk, simulated effluent

Jordana Georgin
Daniel Allasia
Civil Engineering Post Graduation Program,
Federal University of Santa Maria,
Santa Maria 97105-900,
Brazil

Bianca Silva Marques
Enrique Chaves Peres
Guilherme Luiz Dotto (corresponding author)
Chemical Engineering Department,
Federal University of Santa Maria,
Santa Maria 97105-900,
Brazil
E-mail: *guilherme_dotto@yahoo.com.br*

INTRODUCTION

Synthetic dyes are largely employed as coloring agents in the textile, paper, leather, fuel, food, pharmaceutical and other industries (Gupta *et al.* 2013). The majority of synthetic dyes and their degradation products generate environmental concerns, since they are toxic, carcinogenic and recalcitrant molecules (Gupta *et al.* 2015). Dyes can be classified as anionic, cationic or non-ionic (Gupta & Suhas 2009). Crystal violet (CV) is a cationic dye used for dyeing cotton, wool and silk (Khan *et al.* 2015). Methylene blue (MB) in turn, is another cationic dye used for dyeing cotton, paper, wool and silk. It is also used in microbiological diagnostics and is a mesoporosity indicator (Abdallah & Taha 2012). Nowadays, CV and MB are used as indicators in laboratories and volumetric analysis. Since CV and MB are widely used and can cause environmental problems, these dyes should be carefully removed from aqueous effluents.

There are different operations which are used for the treatment of colored effluents, including oxidation, ion exchange, coagulation/flocculation, adsorption on activated carbon, membrane separation, chemical precipitation, biological, photochemical and electrochemical processes (Gupta & Suhas 2009). Adsorption is an accessible and versatile option, but the choice of the adsorbent material can make the process more expensive. Also, most adsorbents cannot be reused or discarded, generating a secondary residue. Alternatively, biosorption, the removal of contaminants from aqueous media by inactive or non-living biomass, has gained attention (Vanni *et al.* 2017). Biosorbents are mainly composed of humic substances, lignin, cellulose, hemicellulose and proteins. These macromolecules contain active sites like hydroxyl, carboxyl and amines, which are able to bind with dyes (Dotto *et al.* 2015a). Some examples of biosorbents are sugarcane bagasse, passion fruit wastes, orange peel, pineapple peel (Dotto *et al.* 2016), *Eragrostis plana* Nees (Dotta-Filho *et al.* 2017), papaya seeds (Weber *et al.* 2014), giombo persimmon seeds (Bretanha *et al.* 2016a) and ouricuri fiber (Meili *et al.* 2017).

Agro-industrial wastes are generated in large volumes, and consequently, their management and disposal are problematic. In this sense, the use of biosorbents based on agro-industrial wastes to remove dyes from aqueous solutions is even more relevant. Pará chestnut (*Bertholletia*

doi: 10.2166/wst.2018.041

excelsa) is a large tree species from Lecythidaceae family, which is native to the Amazonia region (Brazil). This tree can reach 50 m in height and produces spherical fruits containing 12–25 seeds each (Souza & Menezes 2004). Acre, Amazonas and Pará are the most productive states, generating large volumes of chestnut husks (Brito *et al.* 2010). So, alternative uses for chestnut husks are required. Brito *et al.* (2010) studied the adsorption of MB and indigo carmine on raw Brazil nut shells and found adsorption capacities around 8 mg g^{-1}. However, work is still necessary to improve these adsorption capacities and verify the performance regarding the treatment of simulated effluents.

This work focused on the evaluation of Pará chestnut husk (*Bertholletia excelsa*) (PCH) as an alternative biosorbent to remove the cationic dyes CV and MB from aqueous media. PCH was prepared and characterized according to the point of zero charge (pH_{zpc}), X-ray diffraction (XRD), Fourier transform infrared spectroscopy (FT-IR) and scanning electron microscopy (SEM). The effects of biosorbent dosage and initial pH of the solution on the biosorption were studied. Pseudo-first-order (PFO), pseudo-second-order (PSO) and Elovich models were used to study the biosorption kinetics. The equilibrium isotherms were investigated by the Freundlich, Langmuir, and Sips models. PCH was also tested as a biosorbent to treat colored effluents containing several dyes and chemicals.

MATERIALS AND METHODS

Preparation and characterization of PCH biosorbent

Chestnut husks were obtained from a farm located in Rondônia state, Brazil. Husks were washed several times with distilled water and oven dried at 60 °C for 12 hours. Samples were then ground in a knife mill and sieved. Particles smaller than 250 μm were used.

PCH biosorbent was characterized according to the pH_{zpc}, XRD, FT-IR and SEM. The pH_{zpc} was determined using the eleven points experiment (Park & Regalbuto 1995). The amorphous/crystalline structure of PCH was determined by XRD (Rigaku, Miniflex 300, Japan) (Saygılı & Güzel 2016). FT-IR (Shimadzu, Prestige 21, Japan) was used to identify the functional groups on the PCH surface (Silverstein *et al.* 2007). The textural characteristics of PCH were visualized by SEM (Jeol, JSM-6610LV, Japan) (Goldstein *et al.* 1992).

Cationic dyes

CV and MB were selected as target dyes for this study. CV (color index 42555, molar weight of 407.98 g mol^{-1}, $\lambda_{max} = 590$ nm) and MB (color index 52015, molar weight of 319.80 g mol^{-1}, $\lambda_{max} = 664$ nm) were provided by INLAB (Brazil) with a purity higher than 96%. All dye solutions were prepared with distilled water and the reagents were of analytical grade.

Batch biosorption experiments

CV and MB stock solutions were prepared with distilled water and stored in amber flasks. The biosorption experiments were performed by consecutive dilutions of these solutions. The dye concentration in the liquid phase was measured by spectrophotometry at the maximum wavelength for each dye (Biospectro SP-22, Brazil). Experiments were carried out in triplicate using closed vessels, and controls were performed. Biosorption experiments were carried out in batch mode at 200 rpm using a thermostated agitator (Marconi, MA 093, Brazil), and with a fixed volume of solution of 100 mL. After each experiment, the solid-liquid separation was performed by centrifugation (Centribio, 80-2B, Brazil) at 4,000 rpm for 10 min.

Effects of biosorbent dosage and initial pH of the solution on the biosorption were evaluated. Furthermore kinetic and equilibrium curves were constructed. The biosorbent dosage effect was evaluated using 0.5, 0.8, 1.0, 1.5 and 2.0 g L^{-1}, with initial dye concentration of 100 mg L^{-1}, pH of 6.5 and temperature of 25 °C, during 4 hours of agitation. The pH effect was evaluated at 2, 4, 6.5, 8 and 10, with initial dye concentration of 100 mg L^{-1}, biosorbent dosage of 0.5 g L^{-1} and temperature of 25 °C, during 1 hour of agitation. Kinetic curves (contact times of 2, 6, 10, 15, 20, 40, 60, 90 and 120 min) were constructed with initial dye concentrations of 100, 200 and 300 mg L^{-1}, biosorbent dosage of 0.5 g L^{-1} and temperature of 25 °C, using the best pH for each dye. Equilibrium isotherms were obtained at 25, 35, 45 and 55 °C, using initial dye concentrations from 50 to 500 mg L^{-1}, with biosorbent dosage of 0.5 g L^{-1} and under the best pH above determined.

The dye removal percentage (R, %), mass of dye biosorbed per gram of biosorbent at any time (q_t (mg g^{-1})) and at equilibrium (q_e (mg g^{-1})) were calculated as follows:

$$R = \frac{(C_0 - C_e)}{C_0} 100 \quad (1)$$

$$q_t = \frac{(C_0 - C_t)}{W} V \quad (2)$$

$$q_e = \frac{(C_0 - C_e)}{W} V \quad (3)$$

where, C_o, C_t, C_e (mg L^{-1}) are the dye concentrations at $t = 0$, at any time and at equilibrium, respectively, W (g) is the biosorbent amount and V (L) is the volume of the solution.

Kinetic models

The biosorption kinetics of CV and MB on PCH was evaluated by the PFO (Lagergren 1898), PSO (Ho & McKay, 1998) and Elovich models (Zeldowitsch 1934). PFO and PSO models are given by:

$$\frac{dq_t}{dt} = k_1(q_e - q_t) \quad (4)$$

$$\frac{dq_t}{dt} = k_2(q_e - q_t)^2 \quad (5)$$

Solving these equations by variable separation, from $t = 0$ to $t = t$ and from $q_t = 0$ to $q_t = q_e$, and replacing q_e for q_1 or q_2, we have, respectively:

$$q_t = q_1(1 - \exp(-k_1 t)) \quad (6)$$

$$q_t = \frac{t}{(1/k_2 q_2^2) + (t/q_2)} \quad (7)$$

where, k_1 and k_2 are the rate constants of PFO and PSO models, respectively in (min^{-1}) and (g mg^{-1} min^{-1}), q_1 and q_2 are the theoretical values for the biosorption capacity (mg g^{-1}).

The Elovich model, in turn, is given by:

$$q_t = \frac{1}{b} \ln(1 + abt) \quad (8)$$

where, a is the initial velocity due to dq/dt with $q_t = 0$ (mg g^{-1} min^{-1}), b is the desorption constant of the Elovich model (g mg^{-1}) and, t is the time (min).

Isotherm models

CV and MB biosorption on PCH was studied using the Langmuir (Langmuir 1918), Freundlich (Freundlich 1906) and Sips (Sips 1948) isotherm models, as demonstrated:

$$q_e = \frac{q_m K_L C_e}{1 + (K_L C_e)} \quad (9)$$

$$q_e = K_F C_e^{1/n_F} \quad (10)$$

$$q_e = \frac{q_S (K_S C_e)^m}{1 + (K_S C_e)^m} \quad (11)$$

where, q_m is the maximum biosorption capacity (mg g^{-1}), K_L is the Langmuir constant (L mg^{-1}), K_F is the Freundlich constant (mg g^{-1})(mg L^{-1})$^{-1/nF}$, $1/n_F$ is the heterogeneity factor, q_S the maximum biosorption capacity from the Sips model (mg g^{-1}), K_S the Sips constant (L mg^{-1}) and m the Sips exponent. Another important aspect of the Langmuir model is the equilibrium factor, R_L:

$$R_L = \frac{1}{1 + (K_L C_e)} \quad (12)$$

For $R_L = 1$, the isotherm is linear; $0 < R_L < 1$ indicates a favorable process and $R_L = 0$ indicates an irreversible process.

Statistical analysis of the fitted models

The parameters in equations 6 to 11 were estimated by nonlinear regression, minimizing the least squares function and using the Quasi-Newton estimation method. Statistic 9.1 software (Statsoft, USA) was used to perform the calculations. The fit quality was measured through the determination coefficient (R^2), adjusted determination coefficient (R^2_{adj}) and average relative error (ARE) (Dotto *et al.* 2013).

Treatment of simulated textile effluent

Aiming to verify the potential of PCH to treat colored effluents in real conditions, a simulated textile effluent from the dyeing step was generated based on Lima *et al.* (2017). The characteristics of this effluent are presented in Table 1. The effluent (100 mL) was treated with 5 g L^{-1} of PCH at 25 °C for 2 hours. The effluents before and after treatment were submitted to a spectroscopic scanning from 300 to 800 nm. The color removal percentage was found by the ratio between the area above of the spectroscopic curves,

Table 1 | Chemical composition of the simulated textile effluent from the dyeing step

Compounds	λ_{max}	Concentration (mg L^{-1})[a]
Crystal Violet	590	50
Methylene Blue	664	50
Malachite Green	615	10
NaCl	–	100
$NaHCO_3$	–	100
pH	–	7.2

[a]based on Lima *et al.* (2017).

which were obtained using the tool calculus/integrate in origin 2015 software.

RESULTS AND DISCUSSION

Biosorbent characteristics

PCH biosorbent was characterized according to the pH_{zpc}, XRD, FT-IR and SEM. The pH_{zpc} of the biosorbent was 4.8. This indicates that at pH values lower than 4.8, PCH is positively charged, while at pH values higher than 4.8, the biosorbent is negatively charged.

The XRD pattern of the biosorbent is depicted in Figure 1. It can be seen that the PCH biosorbent has a completely amorphous structure. This feature is interesting for biosorption since the empty spaces in the disorganized structure can be occupied by the dye molecules.

The FT-IR spectrum of PCH biosorbent is presented in Figure 2. The main vibrational bands identified were

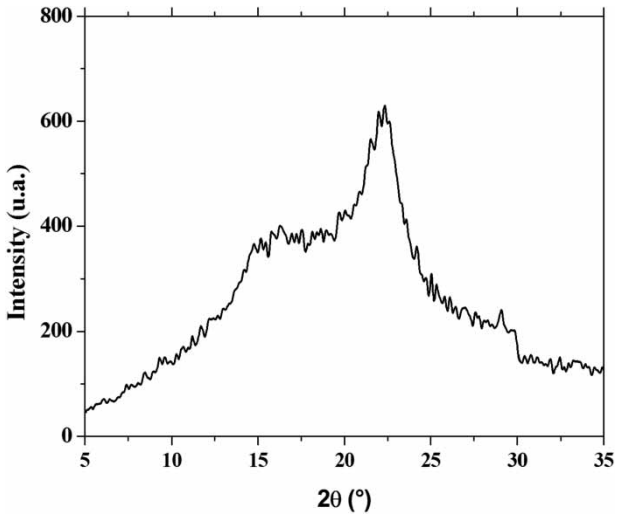

Figure 1 | XRD pattern of the PCH biosorbent.

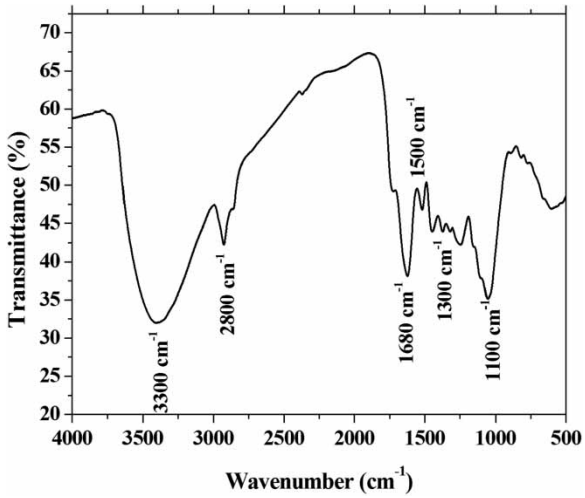

Figure 2 | FT-IR spectrum of the PCH biosorbent.

3,300, 2,800, 1,680, 1,550 and the region 1,300–1,100 cm^{-1}. The band at 3,300 cm^{-1} can be attributed to the -OH stretching vibrations of cellulose, lignin or hemicellulose, which are present in the PCH structure. It could also be OH from adsorbed water. The signal at 2,800 cm^{-1} is related to the C-H links, which are typical of aliphatic compounds and aldehydes. The C = O bond of carboxylic acids, ketones or esters can be related to 1,680 cm^{-1}. C = C links, which can be related with the lipid fraction of PCH, can be seen in 1,500 cm^{-1}. The vibrational bands in the region 1,300–1,100 cm^{-1} are related to the C-O links, which are typical of carbohydrates and phenolic compounds. The FT-IR spectrum revealed that PCH contains several functional groups in the structure, which can be potential biosorption sites for CV and MB dyes.

Figure 3 presents the SEM images of the PCH biosorbent. It can be observed in Figure 3 that the PCH sample was composed of irregular particles ranging in size from 20 to 100 μm. The particles presented an irregular and rough surface. Some cavities were also observed. These characteristics are typical for agro-industrial wastes like papaya seeds (Pavan *et al.* 2014), giombo persimmon seeds (Bretanha *et al.* 2016a) and ouricuri fiber (Meili *et al.* 2017).

Biosorbent dosage effect

The biosorbent dosage effect is presented in Figure 4. Figure 4 shows that the biosorption capacity of CV and MB on PCH was favored by the biosorbent dosage decrease from 2 to 0.5 g L^{-1}. The maximum values were around 55 mg g^{-1} and were attained using 0.5 g L^{-1} of PCH. This behavior is the result of the aggregation of biosorption

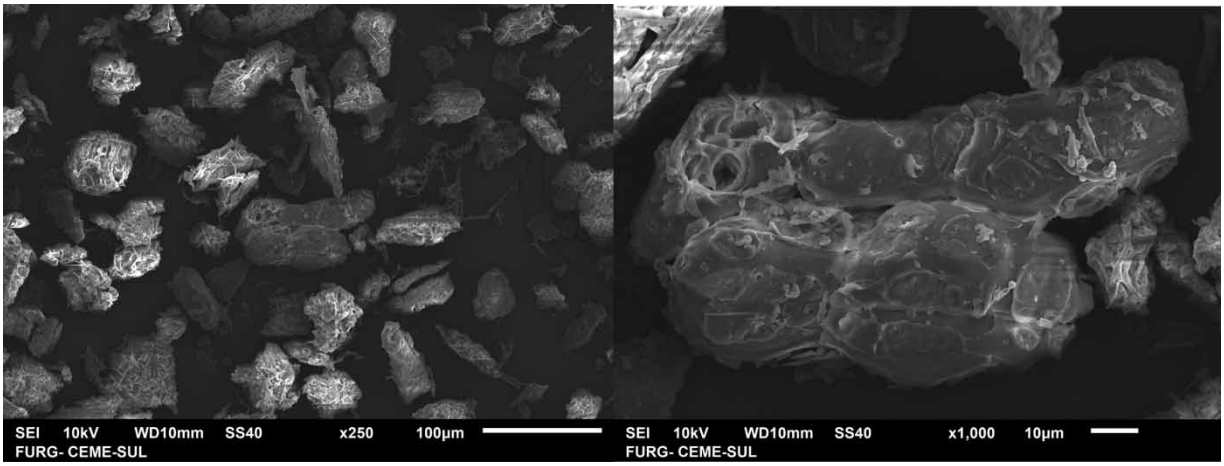

Figure 3 | SEM images of the PCH biosorbent.

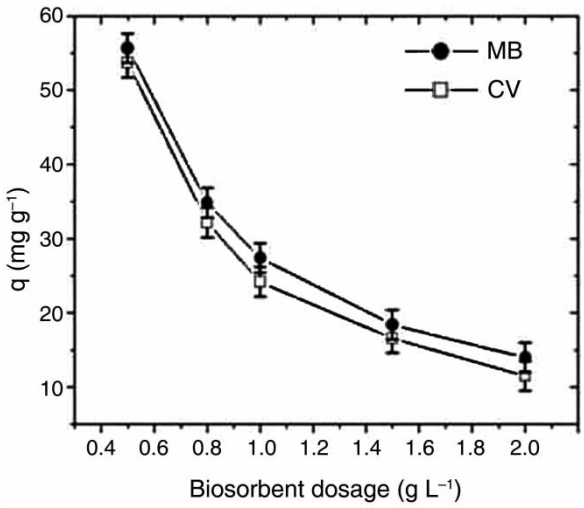

Figure 4 | Effect of biosorbent dosage on the biosorption of CV and MB dyes by PCH ($C_o = 100$ mg L^{-1}, $T = 25$ °C, $t = 4$ hours, $V = 100$ mL, pH = 6.5 and stirring rate = 200 rpm).

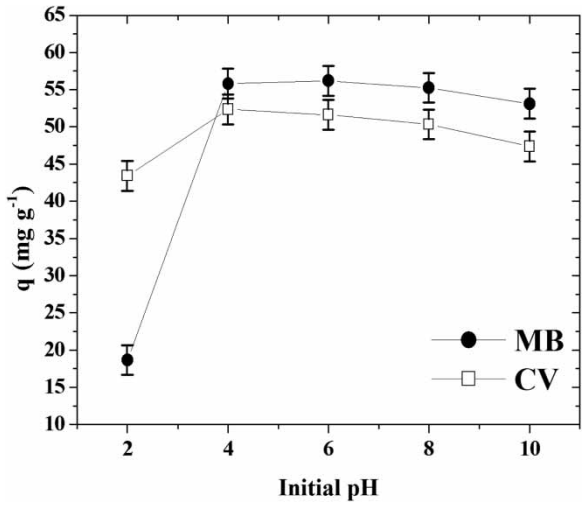

Figure 5 | Effect of initial pH on the biosorption of CV and MB dyes by PCH ($C_o = 100$ mg L^{-1}, $T = 25$ °C, $t = 1$ hour, $V = 100$ mL, biosorbent dosage = 0.5 g L^{-1} and stirring rate = 200 rpm).

sites at higher adsorbent dosages. So, the biosorption sites are not completely used. On the other hand, at low biosorbent dosages, the biosorption sites are effectively occupied. The same trend was found by Meili *et al.* (2017) in the biosorption of MB on ouricuri fiber. Based on these results, the biosorbent dosage of 0.5 g L^{-1} was selected for the subsequent studies.

Ph effect

The effect of initial pH on the biosorption of CV and MB dyes by PCH was evaluated with $C_o = 100$ mg L^{-1}, $T = 25$ °C, $t = 1$ hour, $V = 100$ mL, biosorbent dosage = 0.5 g L^{-1} and stirring rate = 200 rpm. The results are depicted in Figure 5.

For both dyes, it was found that the pH increase from 2 to 4 caused an increase in biosorption capacity, with the maximum values obtained at pH 4. A new increase from 4 to 10 provoked a decrease in biosorption capacity. This behavior is uncommon for cationic dyes, but has already been reported in the literature. Guler *et al.* (2016) also found higher values of biosorption capacity under acid conditions, in the CV biosorption of algae. From 2 to 4, we can infer that at low pH values, there is competition between the H^+ ions and the positively charged dyes MB and CV for the negatively charged biosorption sites ($pH_{zpc} = 4.8$), leading to lower biosorption capacities. This competition decreases when the pH increases, and consequently higher biosorption capacities are obtained. The biosorption capacity decrease from pH 4 to 10 can be

explained as follows: under basic conditions, the lignocellulosic fibers (mainly cellulose and hemicellulose) of PCH can be hydrolyzed, and a fraction of the biosorbent is solubilized. Evidently, this leads to a decrease in biosorption sites. In order to prove this statement, 1 g of biosorbent was added to 100 mL of acid (HCl) and alkaline (NaOH) solutions, and stirred for 1 hour, after which the solutions were left for 40 min. Under acid conditions, 0.98 g of PCH remained solid, demonstrating that the biosorbent is stable at low pH values. However, in alkaline conditions, PCH dissolved and color was released into the solution. In this case, only 0.07 g remained in the solid state. Based on these results, a pH of 4.0 was selected for the subsequent studies of CV and MB biosorption on PCH. It should be highlighted that the biosorbent proposed in this work (PCH) can only be used in acid media, since this material is solubilized at pH values higher than 7.0.

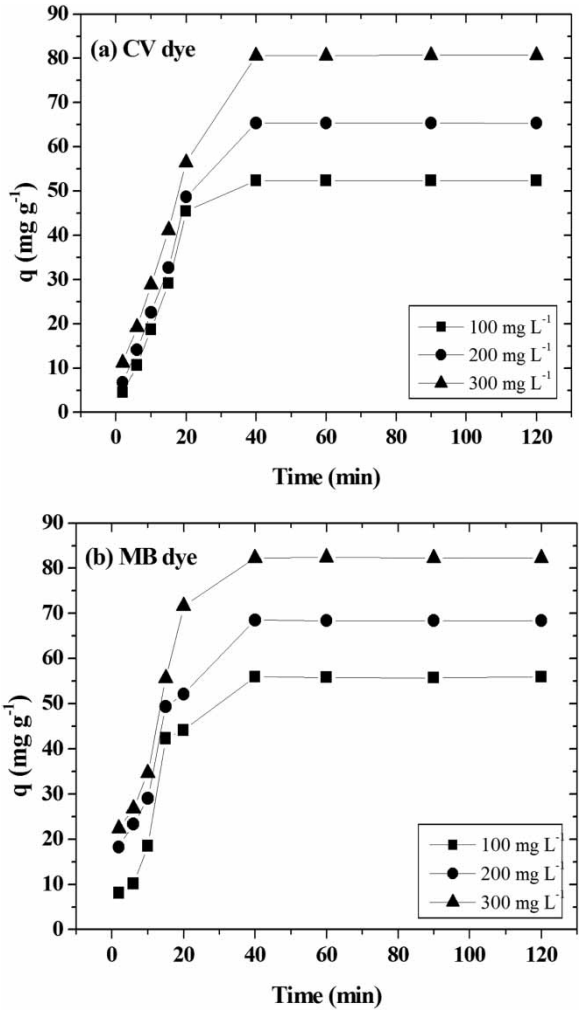

Figure 6 | Biosorption kinetic curves of CV and MB on PCH biosorbent.

Table 2 | Kinetic parameters for the biosorption of CV on PCH

	Initial concentration (mg L^{-1})		
Models	**100**	**200**	**300**
PFO model			
q_1 (mg g^{-1})	54.3	68.0	83.6
k_1 (min^{-1})	0.057	0.051	0.051
R^2	0.9660	0.9804	0.9853
ARE (%)	14.42	8.92	8.88
PSO model			
q_2 (mg g^{-1})	61.8	75.6	88.7
k_2 (g mg^{-1} min^{-1})	0.00124	0.00088	0.00091
R^2	0.9346	0.9511	0.9471
ARE (%)	25.99	17.05	14.68
Elovich model			
b (g mg^{-1})	5.8	6.2	8.0
a (mg g^{-1} min^{-1})	0.0637	0.0486	0.0405
R^2	0.9042	0.9298	0.9399
ARE (%)	26.35	18.82	13.41
q_e *(exp)* (mg g^{-1})	52.5	65.3	81.5

Table 3 | Kinetic parameters for the biosorption of MB on PCH

	Initial concentration (mg L^{-1})		
Models	**100**	**200**	**300**
PFO model			
q_1 (mg g^{-1})	57.6	69.4	83.8
k_1 (min^{-1})	0.062	0.072	0.071
R^2	0.9658	0.9741	0.9729
ARE (%)	14.33	9.16	9.68
PSO model			
q_2 (mg g^{-1})	63.9	67.7	91.9
k_2 (g mg^{-1} min^{-1})	0.00110	0.00190	0.00115
R^2	0.922	0.9232	0.9329
ARE (%)	19.55	14.23	13.61
Elovich model			
b (g mg^{-1})	7.1	14.9	17.4
a (mg g^{-1} min^{-1})	0.0629	0.0622	0.051
R^2	0.8924	0.9389	0.9324
ARE (%)	25.76	12.10	13.12
q_e *(exp)* (mg g^{-1})	56.5	67.0	83.5

Biosorption kinetic curves

The biosorption kinetic results are depicted in Figure 6. For CV dye, an initial fast step occurred for the first 20 min. From 20 to 40 min a lower biosorption rate was observed and finally, equilibrium was reached at 40 min. A similar profile was found for MB, but the initial fast step occurred in the first 10 min and the lower biosorption rate was observed from 10 to 40 min. This is a typical kinetic profile, and occurs because in the earlier stages, the biosorption sites are empty, and during the process these sites are progressively occupied. Also, it can be seen in Figure 6 that the biosorption capacity increased with the initial dye concentration. This occurred because at higher concentrations, more biosorption sites can be occupied, since the process is near to saturation. PFO, PSO and Elovich models were used to represent the kinetic curves. The results are presented in Tables 2 (for CV) and 3 (for MB).

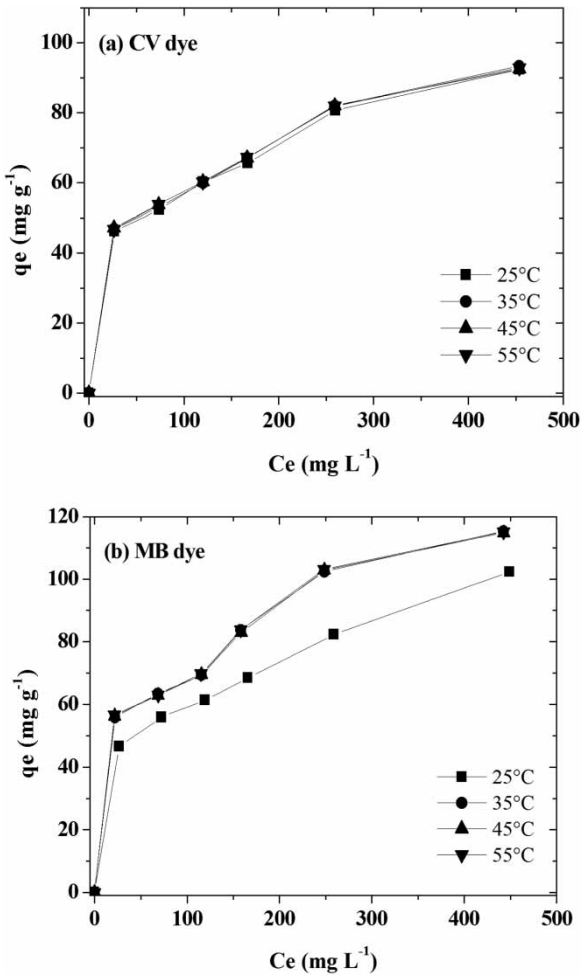

Figure 7 | Biosorption equilibrium curves of CV and MB on PCH biosorbent.

It can be stated that the PFO was better for representing the biosorption of CV and MB on PCH. The R^2 values obtained from this model were superior in relation to PSO and Elovich. Furthermore, the *AREs* were lower for the PFO model. This behavior confirms that the biosorption of CV and MB were fast processes, since the PFO model is mainly suitable for short times (Crini & Badot 2008). The q_1 parameter increased with the initial concentration, reaching maximum values of 83.6 and 83.8 mg g^{-1} for CV and MB, respectively, using 300 mg L^{-1}. In addition, the q_1 parameter was in good agreement with the experimental values ($q_e(exp)$), corroborating the appropriateness of the PFO model for these data. The k_1 parameter ranged from 0.051 to 0.057 for CV, and from 0.062 to 0.072 for MB. The higher k_1 values for MB indicated a faster kinetic for this dye.

Biosorption isotherms

Biosorption equilibrium isotherms are presented in Figure 7. It can be seen that the isotherms were convex,

Table 4 | Isotherm parameters for CV biosorption onto PCH

	Temperature (K)			
Models	**298**	**308**	**318**	**328**
Langmuir				
q_m (mg g^{-1})	90.8	90.8	90.8	90.8
K_L (L mg^{-1})	0.0255	0.0255	0.0255	0.0255
R_L	0.0726	0.0726	0.0726	0.0726
R^2	0.9401	0.9401	0.9401	0.9401
ARE (%)	9.74	9.74	9.74	9.74
R^2_{adj}	0.9281	0.9281	0.9281	0.9281
Freundlich				
K_F ((mg g^{-1})(mg L^{-1})$^{-1/nF}$)	18.2	18.2	18.2	18.2
$1/n_F$	0.2622	0.2622	0.2622	0.2622
R^2	0.9892	0.9892	0.9892	0.9892
ARE (%)	4.50	4.50	4.50	4.50
R^2_{adj}	0.9872	0.9872	0.9872	0.9872
Sips				
q_s (mg g^{-1})	309.4	309.4	309.4	309.4
K_s (L mg^{-1})	0.00014	0.00014	0.00014	0.00014
M	0.33	0.33	0.33	0.33
R^2	0.9872	0.9872	0.9872	0.9872
ARE(%)	4.87	4.87	4.87	4.87
R^2_{adj}	0.9802	0.9802	0.9802	0.9802

Table 5 | Isotherm parameters for MB biosorption onto PCH

	Temperature (K)			
Models	**298**	**308**	**318**	**328**
Langmuir				
q_m (mg g^{-1})	102.9	117.2	117.2	117.2
K_L (L mg^{-1})	0.0174	0.0209	0.0209	0.0209
R_L	0.1026	0.0872	0.0872	0.0872
R^2	0.9271	0.9201	0.9201	0.9201
ARE (%)	10.01	11.78	11.78	11.78
R^2_{adj}	0.9121	0.9041	0.9041	0.9041
Freundlich				
K_F ((mg g^{-1})(mg L^{-1})$^{-1/nF}$)	14.7	19.4	19.4	19.4
$1/n_F$	0.3113	0.2921	0.2921	0.2921
R^2	0.9874	0.9812	0.9812	0.9812
ARE (%)	4.15	5.94	5.94	5.94
R^2_{adj}	0.9854	0.9782	0.9782	0.9782
Sips				
q_s (mg g^{-1})	340.5	407.6	407.6	407.6
K_s (L mg^{-1})	0.00020	0.00015	0.00015	0.00015
m	0.384	0.36	0.36	0.36
R^2	0.9832	0.9781	0.9781	0.9781
ARE (%)	4.49	6.39	6.39	6.39
R^2_{adj}	0.9702	0.9671	0.9671	0.9671

with an inclined portion at lower concentrations, tending to a plateau at higher concentrations. Saturation was not observed in this range of concentrations. We can conclude that PCH possesses several available sites for CV and MB dye. For CV dye, the biosorption was not temperature dependent. However for MB, the temperature

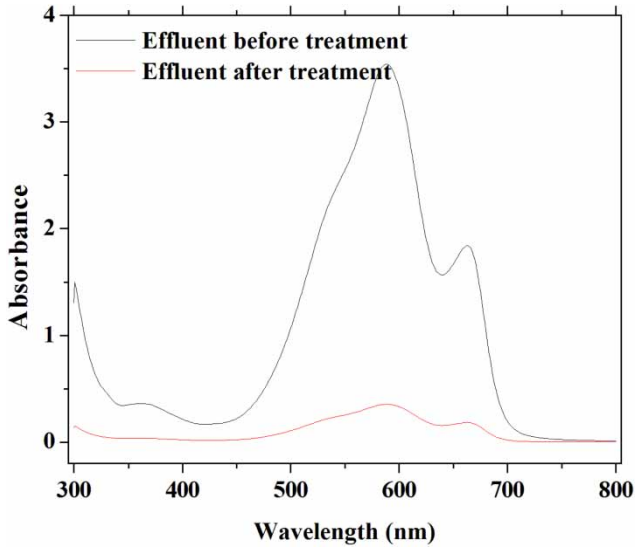

Figure 8 | Visible spectra of textile effluents before and after the biosorption with PCH.

increase from 25 °C to 35 °C favored the biosorption process. New increases to 45 °C and 55 °C had no effect.

To better understand the biosorption equilibrium, Langmuir, Freundlich and Sips isotherm models were fitted to the experimental data. The results are presented in Tables 4 and 5. Based on the values of R^2, R^2_{adj} and *ARE* presented in Tables 4 and 5, it can be stated that the Freundlich model was better for representing the biosorption of CV and MB onto PCH. The Freundlich constant values presented in Table 4 were equal, independent of the temperature. This confirms that the CV biosorption on PCH was not temperature dependent. On the other hand, for MB (Table 5), the K_F value increased from 14.7 to 19.4 with the temperature increase, suggesting that biosorption of MB was favored at 35–

Table 6 | Comparison between the maximum biosorption capacities (q_{max}) of several materials used to remove CV and MB dyes from aqueous solutions

Biosorbent	**Dye**	**pH**	**T (°C)**	**q_{max} (mg g^{-1})**	**Reference**
Pará chestnut husk	CV	4.0	25	83.6	This work
Eragrostis plana Nees	CV	8.0	35	76.20	Dotta-Filho *et al.* (2017)
Papaya seeds	CV	8.0	25	85.99	Pavan *et al.* (2014)
ZSM5-zeolite	CV	8.0	55	141.8	Brião *et al.* (2017)
Modified spirulina	CV	2.0	25	101.87	Guler *et al.* (2016)
Pará chestnut husk	MB	4.0	25	83.8	This work
Ouricuri fibers	MB	5.5	25	31.7	Meili *et al.* (2017)
Punica granatum husk	MB	5.0	25	68.4	Bretanha *et al.* (2016b)
Modified chitin	MB	10.0	25	26.29	Dotto *et al.* (2015b)
Raw chitin	MB	10.0	25	12.52	Dotto *et al.* (2015b)

55 °C. The potential of PCH to remove CV and MB from aqueous solutions was compared with other materials, as presented in Table 6. The results revealed that PCH can be an option for removing these dyes from aqueous solutions, since the biosorption capacities are within the range in the literature.

Potential of PCH to treat textile effluents

The potential of PCH to treat a simulated textile effluent from the dyeing step was verified. The characteristics of this effluent are presented in Table 1. The effluent (100 mL) was treated by 5 g L^{-1} of PCH at 25 °C for 2 hours. The results were quantified in terms of color removal. The visible spectra of the effluent before and after the treatment are shown in Figure 8. The areas under the curves were, respectively, 509.05 and 50.905 for the effluents before and after the treatment. This corresponds to 90% color removal. In this sense, we can conclude that PCH has potential to treat a simulated textile effluent from the dyeing step, which contains several dyes and chemicals.

CONCLUSION

The potential of PCH as an alternative biosorbent to remove CV and MB dyes from aqueous effluents was investigated in this research. PCH presented an amorphous structure with some important functional groups, which were able to take up CV and MB. The biosorption capacities of CV and MB were favored using 0.5 g L^{-1} of PCH at pH 4.0. PCH has the potential to be applied only in acid conditions, since dissolution occurs at high pH values. The PSO model was suitable for representing the biosorption kinetics, since the processes were fast, attaining the equilibrium within 40 min. The equilibrium isotherms were well represented by the Freundlich model. The maximum biosorption capacities were 83.6 and 83.8 mg g^{-1} for CV and MB, respectively. In the treatment of a textile effluent containing several dyes and chemicals, 5 g L^{-1} of PCH provided a color removal of 90%. Thus, PCH can be considered an alternative material to treat textile effluents.

REFERENCES

Abdallah, S. & Taha, S. 2012 Biosorption of methylene blue from aqueous solution by nonviable *Aspergillus fumigates*. *Chemical Engineering Journal* **15** (1), 195–196.

Bretanha, M. S., Dotto, G. L., Vaghetti, J. C. P., Dias, S. L. P., Lima, E. C. & Pavan, F. A. 2016a Giombo persimmon seed (GPS) an alternative adsorbent for the removal Toluidine Blue dye from aqueous solutions. *Desalination and Water Treatment* **57** (58), 28474–28485.

Bretanha, M. S., Rochefort, M. C., Dotto, G. L., Lima, E. C., Dias, S. L. P. & Pavan, F. A. 2016b Punica granatum husk (PGH), a powdered biowaste material for the adsorption of methylene blue dye from aqueous solutions. *Desalination and Water Treatment* **57** (1), 3194–3204.

Brião, G. V., Jahn, S. L., Foletto, E. L. & Dotto, G. L. 2017 Adsorption of crystal violet dye onto a mesoporous ZSM-5 zeolite synthetized using chitin as template. *Journal of Colloid and Interface Science* **508** (1), 313–322.

Brito, S. M. O., Andrade, H. M. C., Soares, L. F. R. & Azevedo, P. 2010 Brazil nut shells as a new biosorbent to remove methylene blue and índigo carmine from aqueous solutions. *Journal of Hazardous Materials* **174** (1), 84–92.

Crini, G. & Badot, P. M. 2008 Application of chitosan, a natural aminopolysaccharide, for dye removal from aqueous solutions by adsorption processes using batch studies: a review of recent literature. *Progress in Polymer Science* **33** (4), 399–447.

Dotta-Filho, E. C., Mazzocato, A. C., Dotto, G. L., Thue, P. S. & Pavan, F. A. 2017 *Eragrostis plana* Nees as a novel eco-friendly adsorbent for removal of crystal violet from aqueous solutions. *Environmental Science Pollution Research* **24** (1), 19909–19919.

Dotto, G. L., Costa, J. A. V. & Pinto, L. A. A. 2013 Kinetic studies on the biosorption of phenol by nanoparticles from *Spirulina* sp. LEB 18. *Journal of Environmental Chemical Engineering* **1** (4), 1137–1143.

Dotto, G. L., Sharma, S. K. & Pinto, L. A. A. 2015a *Biosorption of organic dyes: Research opportunities and challenges*. In: *Green Chemistry for Dyes Removal From Waste Water: Research Trends and Applications* (S. K. Sharma, ed.). John Wiley & Sons, Beverly, USA.

Dotto, G. L., Santos, J. M. N., Rodrigues, I. L., Rosa, R., Pavan, F. A. & Lima, E. C. 2015b Adsorption of Methylene Blue by ultrasonic surface modified chitin. *Journal of Colloid and Interface Science* **446** (1), 133–140.

Dotto, G. L., Meili, L., Abud, A. K. S., Tanabe, E. H., Bertuol, D. A. & Foletto, E. L. 2016 Comparison between Brazilian agro-wastes and activated carbon as adsorbents to remove Ni(II) from aqueous solutions. *Water Science and Technology* **73** (11), 2713–2721.

Freundlich, H. 1906 Uber die adsorption in Losungen. *Zeitschrift fur Physikalische Chemie* **57** (A), 358–471.

Goldstein, J. I., Newbury, D. E., Echil, P., Joy, D. C., Romig Jr., A. D., Lyman, C. E., Fiori, C. & Lifshin, E. 1992 *Scanning Electron Microscopy and X-ray Microanalysis*. Plenum Press, New York, USA.

Guler, U. A., Mehtap, E., Tuncela, E. & Feride, D. 2016 Mono and simultaneous removal of crystal violet and safranin dyes from aqueous solutions by HDTMA-modified *Spirulina* sp. *Process Safety and Environmental Protection* **99** (1), 194–206.

Gupta, V. K. & Suhas, I. 2009 Application of low-cost adsorbents for dye removal-a review. *Journal of Environmental Management* **90** (8), 2313–2342.

Gupta, V. K., Kumar, R., Nayak, A., Saleh, T. A. & Barakat, M. A. 2013 Adsorptive removal of dyes from aqueous solution onto carbon nanotubes: a review. *Advances in Colloid and Interface Science* **193–194** (1), 24–34.

Gupta, V. K., Khamparia, S., Tyagi, I., Jaspal, D. & Malviya, A. 2015 Decolorization of mixture of dyes: a critical review. *Global Journal of Environmental Science Management* **1** (1), 71–94.

Ho, Y. S. & McKay, G. 1998 Kinetic models for the sorption of dye from aqueous solution by wood. *Process Safety and Environmental Protection* **76** (B2), 183–191.

Khan, T. A., Khan, E. A. & Shahjahan, A. 2015 Removal of basic dyes from aqueous solution by adsorption onto binary iron–manganese oxide coated kaolinite: non-linear isotherm and kinetics modeling. *Applied Clay Science* **107** (1), 70–77.

Lagergren, S. 1898 About the theory of so-called adsorption of soluble substances. *Kungliga Svenska Vetenskapsakademiens* **24** (4), 1–39.

Langmuir, I. 1918 The adsorption of gases on plane surfaces of glass, mica and platinum. *Journal of the American Chemical Society* **40** (9), 1361–1403.

Lima, D. R., Klein, L. & Dotto, G. L. 2017 Application of ultrasound modified corn straw as adsorbent for malachite green removal from synthetic and real effluents. *Environmental Science Pollution Research* **24** (1), 21484–21495.

Meili, L., Silva, T. S., Henrique, D. C., Soletti, J. I., Vieira de Carvalho, S. H., Fonseca, E. J. S., Almeida, A. R. F. & Dotto, G. L. 2017 Ouricuri (*Syagrus coronata*) fiber: a novel biosorbent to remove methylene blue from aqueous solutions. *Water Science and Technology* **75** (1), 106–114.

Park, J. & Regalbuto, J. R. 1995 A simple, accurate determination of oxide PZC and the strong buffering effect of oxide surfaces at incipient wetness. *Journal of Colloid and Interface Science* **175** (1), 239–252.

Pavan, F. A., Camacho, E. S., Lima, E. C., Dotto, G. L., Branco, V. T. A. & Dias, S. L. P. 2014 Formosa papaya seed powder (FPSP): preparation, characterization and application as an alternative adsorbent for the removal of crystal violet from aqueous phase. *Journal of Environmental Chemical Engineering* **2** (1), 230–238.

Saygılı, H. & Güzel, F. 2016 High surface area mesoporous activated carbon from tomato processing solid waste by zinc chloride activation: process optimization, characterization and dyes adsorption. *Journal of Cleaner Production* **113** (1), 995–1004.

Silverstein, R. M., Webster, F. X. & Kiemle, D. J. 2007 *Spectrometric Identification of Organic Compounds*. John Wiley & Sons, New York, USA.

Sips, R. 1948 On the structure of a catalyst surface. *Journal of Chemical Physics* **16** (1), 490–495.

Souza, M. L. & Menezes, H. C. 2004 Processamentos de amêndoa e torta de castanha-do-Brasil e farinha de mandioca: parâmetros de qualidade (*in Portuguese*). *Ciência e Tecnologia de Alimentos* **24** (1), 120–128.

Vanni, G., Escudero, L. B. & Dotto, G. L. 2017 Powdered grape seeds (PGS) as an alternative biosorbent to remove pharmaceutical dyes from aqueous solutions. *Water Science and Technology* **76** (5), 1177–1187.

Weber, C. T., Collazzo, G. C., Mazutti, M. A., Foletto, E. L. & Dotto, G. L. 2014 Removal of hazardous pharmaceutical dyes by adsorption onto papaya seeds. *Water Science and Technology* **70** (1), 102–107.

Zeldowitsch, J. 1934 Über den mechanismus der katalytischen oxydation von CO an MnO_2. *Acta Physicochemical URSS* **1** (3–4), 449–464.

First received 27 September 2017; accepted in revised form 16 January 2018. Available online 30 January 2018